

Analysis on the Calculation of the Inverse Discrete Fourier Transform (IDFT) of Passband Frequency Response Measurements in Terms of Lowpass Equivalent Response

Angelo Gifuni* and Stefano Perna

Abstract—An analysis on the calculation of the inverse discrete Fourier transform (IDFT) of passband frequency response measurements in terms of lowpass equivalent responses is shown, in order to specify the differences in the results given from different common algorithms; differences with respect to the calculation of the IDFT for true lowpass responses are remarked. It is shown how the basic sequence has to be represented in time domain by invoking the causality, which is supported by results. Results are corroborated by an application on measured data in a reverberation chamber. The present analysis helps readers understand different IDFT algorithms used by Manufacturers and make their own codes whenever desirable.

1. INTRODUCTION

Measurements can be made in time domain (TD) [1] and frequency domain (FD) [2]; if it is necessary, measurements made in TD domain can be transformed in FD and vice versa [3] by applying the discrete Fourier transform (DFT) and inverse discrete Fourier transform (IDFT), respectively, which are powerful tools in the engineering field [4–8]. The transformation operations are discrete as it is assumed that the measurements are sampled as is normally the case. Options for real TD measurements using a true radiofrequency pulse (RP) there exist for vector network analyzers (VNAs); but, measurements from VNAs are normally made in FD and it is in some cases necessary to transform them in TD [9–11]. Even though the results in this paper apply to all vectorial measurements made in FD, we almost always will refer to VNA measurements as VNAs are main instruments to make FD vectorial measurements. In a normal IDFT operation the frequency points are harmonically related from the zero frequency point, which corresponds to the direct current (DC) value, to the stop frequency. Since VNAs do not measure the frequency $f_0 = 0$, as well as all frequencies less than their working minimum frequency (WMF), which is always greater than zero, they are extrapolated. Strictly, it implies that the step frequency. Δf is to be such that $f_0 = 0$, $f_1 = \Delta f$, $f_2 = 2\Delta f$, \dots , $f_{start} = k\Delta f$, \dots , $f_{stop} = (M - 1)\Delta f$, where k is an integer number. The frequency response for the negative frequencies is calculated by considering the Hermitian condition; it is because TD values have to be real [4–8], and since TD values are derived from measurements, they turn out to be causal as well [4, 6] except the periodicity due to the sampling. Such a normal method, which is called “lowpass mode” by Manufacturers of VNAs [12–15], actually simulates the traditional time domain reflectometer (TDR); therefore, the type of reactance of an impedance can be determined in TD [12–15]. Note that for lowpass responses, which range from zero to stop frequency, the negative frequencies redouble the frequency range and consequently the resolution in TD. When the measurements are centered between the start and stop frequencies, where the start frequency is distant from the WMF of the VNA, so that any extrapolation for low frequencies and DC component becomes critical in approximation terms apart from the WMF value, then the IDFT has to be applied only to

Received 17 August 2017, Accepted 26 October 2017, Scheduled 26 November 2017

* Corresponding author: Angelo Gifuni (angelo.gifuni@uniparthenope.it).

The authors are with the Dipartimento di Ingegneria, Università degli Studi di Napoli “Parthenope”, Napoli 80143, Italy.

the measured frequency points; this case is called “passband mode” by Manufacturers of VNAs [12–15]. An incident RP is de facto synthesized by the VNA. In this case, more than one algorithm could be used to calculate the IDFT; we will compare three different procedures (algorithms). The IDFT of passband frequency responses is necessarily made by the IDFT of lowpass equivalent responses. However, such TD complex responses derived from IDFT are uniquely transformable in FD again. IDFT operations are implemented in the time domain option of VNAs, but the algorithms used by Manufacturers are not made known to the Customers [12–16]. Nevertheless, such operations can be implemented by users whenever they want to have totally the data processing within their own control for any possible reasons or when it is convenient to process data off line, as it occurs in research activities. The paper helps professionals and researchers in the comprehension and choice of the algorithm which can be used for the IDFT calculation. It is shown why a simple algorithm, which is available in the common software such as MATLAB and LabVIEW, can normally be used for such a scope. It is also shown how the basic sequence has to be represented in TD. The analysis made in this paper also remarks the differences that there exist between the calculation procedures of the IDFT for lowband and passband responses. A meaningful application of the IDFT on measurements made inside a reverberation chamber (RC) is shown and discussed to corroborate the results; the invoked causality is also supported by measurements.

2. IDFT ANALYSIS ON THE CALCULATION OF PASSBAND FREQUENCY RESPONSES IN TERMS OF LOWPASS EQUIVALENT RESPONSES

The calculation of the IDFT, as well as that of the DFT, is normally made by the more fast algorithms for the inverse fast Fourier transform I-FFT and FFT, respectively. However, this does not invalidate the goal of this paper. The frequency responses are sampled and inevitably broken off; therefore, the responses to be processed are sequences. The truncation and the sampling make the response periodic, in both domains; they cause ringing and aliases, respectively. However, they are not examined below. Moreover, for the goal of the paper, it is sufficient to consider a rectangular window for data processing. Even though the real algorithms used by Manufacturers of VNAs are not made known to the Customers, for passband frequency responses, they say that the IDFT is applied from minus one-half of the frequency span to plus one-half of the frequency span itself [12–14]. Span frequency is the difference between stop frequency and start frequency; that is, $f_{span} = f_{stop} - f_{start}$. In [13], it is specified that the sequence transformed in TD ranges from $-T/2$ to $T/2$, where $T = 1/\Delta f$, and Δf is the step frequency; it is de facto selected during the calibration procedure of a VNA. However, by also considering the reference planes due to the calibration, it does not satisfy the causality apart from the periodicities due to the sampling; therefore, we use a basic sequence transformed in TD that ranges from 0 to T as shown below. In order to calculate the IDFT of passband frequency responses, we first show a procedure where negative and positive frequencies are requested. A passband frequency response can be processed as an unsymmetrical passband signal [4–6], which has a Hermitian symmetry as the response in TD is real; it is also causal. From measured response, we can easily obtain the part negative of the spectrum. Both negative and positive parts of the spectrum can be shifted in frequency so that the equivalent low pass response can be achieved. We first consider a frequency shift $f_c = (f_{start} + f_{stop})/2$ so that the corresponding low pass equivalent response is centered at $f_0 = 0$. We develop the calculation procedure by considering a scattering coefficient as a measured frequency response, which is denoted by $S(f_{start} + n\Delta f)$; n is an integer that ranges from 0 to $N - 1$. N is the amplitude of the measured sequence; it turns out that $N - 1 = (f_{stop} - f_{start})/\Delta f$. The measured frequency response includes only positive frequencies, which range from f_{start} to f_{stop} ; the negative frequencies, which range from $-f_{start}$ to $-f_{stop}$, are obtained by as follows:

$$S(f_n) = \begin{cases} S_2(-f_{start} - n\Delta f) & \text{if } f_n = (-f_{start} - n\Delta f) \\ S_1(f_{start} + n\Delta f) & \text{if } f_n = (f_{start} + n\Delta f) \\ \text{It is not defined elsewhere} & \end{cases}, \quad (1a)$$

where

$$S_2(-f_{start} - n\Delta f) = \frac{S^*(f_{start} + n\Delta f)}{2}, \quad (1b)$$

$$S_1(f_{start} + n\Delta f) = \frac{S(f_{start} + n\Delta f)}{2}. \quad (1c)$$

The symbol * means complex conjugate. Note that when $n = 0$, $-f_{start} - n\Delta f = -f_{start}$ and $f_{start} + n\Delta f = f_{start}$, whereas when $n = N - 1$, $-f_{start} - n\Delta f = -f_{stop}$ and $f_{start} + n\Delta f = f_{stop}$. In order to calculate the IDFT of the frequency response, the negative and positive responses are shifted to $f_0 = 0$; that is, S_2 is shifted of f_c and S_1 is shifted of $-f_c$. After such a shift, S_2 and S_1 are denoted by $S_{2,l}$ and $S_{1,l}$, where the subscript l means equivalent low pass frequency response. The frequencies of $S_{2,l}$ and $S_{1,l}$ range from $-f_{span}/2$ to $f_{span}/2$. The in-phase and quadrature components of the frequency response can be obtained. We can write:

$$S_p(-f_{span}/2 + n\Delta f) = \frac{S_{2,l}(-f_{span}/2 + n\Delta f) + S_{1,l}(-f_{span}/2 + n\Delta f)}{2}, \quad (2a)$$

$$S_q(-f_{span}/2 + n\Delta f) = \frac{S_{2,l}(-f_{span}/2 + n\Delta f) - S_{1,l}(-f_{span}/2 + n\Delta f)}{2i}, \quad (2b)$$

where the subscripts p and q mean in-phase and quadrature components, respectively, whereas i denotes the imaginary unit. It can be shown that S_p and S_q have Hermitian symmetry [4, 6]. The IDFT of S_p and S_q , which have real values, can be calculate as follows:

$$s_p(m\Delta t) = \frac{1}{M} \sum_{J=-(N-1)/2}^{J=(N-1)/2} S_p(J\Delta f) e^{i2\pi Jm/M}, \quad (3a)$$

$$s_q(m\Delta t) = \frac{1}{M} \sum_{J=-(N-1)/2}^{J=(N-1)/2} S_q(J\Delta f) e^{i2\pi Jm/M}, \quad (m = 0, 1, \dots, M - 1 = N - 1), \quad (3b)$$

where M is the number of time points; Δt is the step time; $s(m\Delta t)$ is the response in TD. It is specified that $M = N$ for bandpass frequency response. Note that Eq. (3) includes only natural window (rect. window), which is our case as we do not apply different windows. Note that in Eq. (3) the time $m\Delta t$ ranges from 0 to T . Equations (3) give the TD sequence concerning the complex envelope of the measured frequency response; therefore, they normally give complex values in TD. The complex representation in TD does not invalidate the causality principle. However, the TD response corresponding to the passband response is a real function [4–6]. The span frequency determines the minimum resolution in time, which is equal to $\Delta t = 1/(\Delta f(M - 1))$; the latter, along with the window type applied to data, determines the resolution in TD as shown by Equations (4) and (5) below. We can write:

$$s_p(m\Delta t) - is_q(m\Delta t) \leftrightarrow S_{1,l}(-f_{span}/2 + n\Delta f), \quad (4a)$$

$$s_q(m\Delta t) + is_p(m\Delta t) \leftrightarrow S_{2,l}(-f_{span}/2 + n\Delta f), \quad (m, n = 0, 1, \dots, M - 1 = N - 1), \quad (4b)$$

where the symbol \leftrightarrow denotes Fourier transform pair. The envelope and phase of the response, which are denoted by $A(m\Delta t)$ and $\phi(m\Delta t)$, respectively, can be simply obtained as follows [4]:

$$A(m\Delta t) = 2\sqrt{s_p^2(m\Delta t) - s_q^2(m\Delta t)}, \quad (5a)$$

$$\phi(m\Delta t) = \tan^{-1} \left(\frac{s_q(m\Delta t)}{s_p(m\Delta t)} \right). \quad (5b)$$

Note that lowband responses are always symmetrical, whereas passband responses are normally unsymmetrical. However, if a passband response is symmetrical, the quadrature component turns out to be zero and the procedure in Eqs. (1)–(3) gives a real signal in TD. It is because the corresponding lowpass equivalent response has also Hermitian symmetry. The time resolution is the same for both symmetrical and unsymmetrical passband responses, whereas it is doubled for lowpass responses with the same measured frequency range. To achieve the IDFT of the bandpass response, which is real, we can use the in-phase and quadrature components and apply the modulation theorem [4–6]. However, since we are dealing with IDFT of equivalent lowpass responses, to correctly represent the bandpass response in TD, it is generally necessary to interpolate and resample the in-phase and quadrature components appropriately, as shown in [17] and in references therein. Note that when $f_{start} = I \cdot f_{span}$, where I is an integer number, no interpolation and resampling is necessary [17]. We do not show further details on the procedure to achieve the bandpass response in TD as it is not of interest for this study.

An equivalent method can be used to obtain the IDFT of equivalent low pass responses; in fact, the measured response $S(f_{start} + n\Delta f)$ can be considered as the DFT of the analytic response associated with $S(f_n)$ [5, 8]. The analytic response includes only the positive frequency as its imaginary part is the Hilbert transform of the real part. Therefore, the measured response can be simply shifted of $-f_c$, and the following algorithm can be applied:

$$s_{-f_c}(m\Delta t) = \frac{1}{M} \sum_{J=-(N-1)/2}^{J=(N-1)/2} S_{-f_c}(J\Delta f) e^{i2\pi Jm/M}, \quad (m = 0, 1, \dots, M-1 = N-1), \quad (6)$$

where S_{-f_c} and s_{-f_c} are the measured frequency response shifted of $-f_c$ and the corresponding IDFT, respectively. It can be noted that $s_{-f_c}(m\Delta t) = 2s_p(m\Delta t) - i2s_q(m\Delta t)$ as expected; in other words, the real and imaginary parts of the IDFT given by Eq. (6) are twice of the corresponding values of $s_p(m\Delta t)$ and $s_q(m\Delta t)$ given by Eqs. (3a) and (3b), respectively. By algorithm in Eq. (6), the in-phase and quadrature components given by previous procedure are de facto obtained again, and Eqs. (5a) and (5b) can be applied again. Therefore, the procedures in Eqs. (3) and (6) are equivalent; we can write:

$$2s_p(m\Delta t) - i2s_q(m\Delta t) \leftrightarrow S_{-f_c}(-f_{span}/2 + n\Delta f) = 2S_{1,l}(-f_{span}/2 + n\Delta f). \quad (7)$$

When N is even, $(N-1)/2$ is not an integer; in these cases, in Eqs. (3) and (6), as well as in Eq. (2) and consequently Eq. (4), the shift f_c can become $f_c + \Delta f/2$, and the shift $-f_c$ can become $-f_c - \Delta f/2$ so that the frequencies $f_c + \Delta f/2$ and $-f_c - \Delta f/2$ in the positive and negative part of the response are shifted to $f = 0$. Alternatively, the shift f_c can become $f_c - \Delta f/2$, and the shift $-f_c$ can become $-f_c + \Delta f/2$. The difference between the two choices is a light shift in the phase of the TD response, which does not invalidate the calculation procedures. Note that Eq. (6) includes suggestions of Manufacturers of VNAs except for the range of the sequence in TD [13], as specified above. The equivalent low pass responses shown above are not unique. They depend on the frequency shift, which is $-f_c$, f_c , and $-f_c$ in the cases considered above.

Another procedure to calculate the IDFT of passband frequency responses is the basic algorithm used in common software (such as MATLAB and LabVIEW); it is as follows:

$$s_{-f_{start}}(m\Delta t) = \frac{1}{M} \sum_{n=0}^{n=N-1} S_{-f_{start}}(n\Delta f) e^{i2\pi nm/M}, \quad (m = 0, 1, \dots, M-1 = N-1), \quad (8)$$

where $S_{-f_{start}}$ and $s_{-f_{start}}$ are the measured frequency response shifted of $-f_{start}$ and the corresponding IDFT, respectively. Note that the equivalent low pass response in Eq. (8), where the frequencies are shifted of f_{start} , as well as that in Eq. (6), is an analytic response shifted to the low frequencies. The negative frequencies can also be obtained in this case, and equations all similar to Eqs. (2a) and (2b) can be applied to achieve the DFT of the corresponding in-phase and quadrature components. When the algorithm in Eq. (8) is used for the IDFT, the concerning envelope is the same as those given in Eq. (5a) and by Eq. (6), but the phase given by Eq. (8) is different by the phase given by Eq. (5b); it is because the shifts in frequency are different as shown above. For a right comparison between the corresponding in-phase and quadrature components, the specific frequency shift has to be considered and it is generally necessary to interpolate and resample the components appropriately [17]. In other words, the comparisons between two TD sequences corresponding to two different frequency shifts is not achieved by simply multiplying a response by a complex exponential depending on $m\Delta t$. It is finally remarked that considering that the TD complex responses derived from IDFT are uniquely transformable in FD again, only the TD complex envelope is usually necessary for applications. Accordingly, in most cases, a phase difference between the expressions in Eqs. (8) and (5b) can be safely accepted. Therefore, the algorithm in Eq. (8), which is the simplest and the most available in commercial software routines, can be favourably used whenever desirable.

3. APPLICATIONS TO MEASUREMENTS

The algorithms in Eqs. (3), (6), and (8) are applied to measurements made in an RC. The RC used for the measurements is a cubic chamber of 8 m^3 volume, where the input electromagnetic field is randomized by means of three metallic stirrers rotating in continuous mode as described in [18–20]. A

two-port VNA, Agilent model 8363B is used for measurements. The measurement setup includes two equal double-ridge waveguide horn antennas, ETS-Lindgren model 3115. A full two-port calibration using an unknown thru was made and all four scattering parameters were measured by acquiring 16,001 frequency points from 1 GHz to 18 GHz. Hence, $\Delta f = 1.0625$ MHz, $\Delta t = 0.0588$ ns, and TD ranges from 0 to 941.18 ns. Fig. 1 shows the amplitude of the measured transmission coefficient S_{21} or equivalently S_{12} .

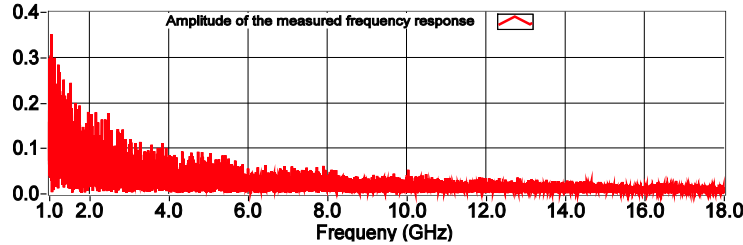


Figure 1. Amplitude of the transmission coefficient measured in an RC.

Figure 2(a) shows the amplitude of the measured transmission coefficient (in FD) shifted of $-f_c$ along with the frequency responses achieved by applying the DFT to the TD sequence derived by IDFT in Eqs. (3) and (6). In other words, the FD traces concerning the algorithms in Eqs. (3) and (6) are obtained again, in order to show the DFT pair and to highlight that the TD traces correspond to complex envelopes of the measured response. The three traces are perfectly overlapped, as expected.

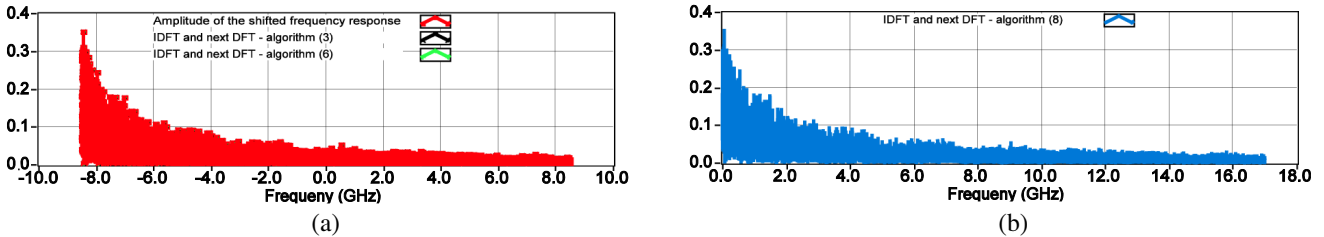


Figure 2. (a) The red trace is the amplitude of the transmission coefficient measured in the RC and shifted of $-f_c$. The black and green traces are the amplitudes of the DFT of the complex envelopes concerning the algorithms in Eqs. (3) and (6), respectively. The three traces are perfectly overlapped. (b) Amplitude of the DFT of the complex envelope concerning the transmission coefficient measured in the RC and processed by the algorithm in Eq. (8).

Figure 2(b) shows the amplitude of the TD traces concerning the complex envelopes derived by applying the algorithm in Eq. (8). The traces concerning the algorithms in Eqs. (3) and (6) and that concerning the algorithm in Eq. (8) have been represented in different planes to remark the fact that they derive from different complex envelopes. In fact, the spectrums of the complex envelopes concerning the algorithms in Eq. (3) and (6) range from -8.5 GHz to 8.5 GHz whereas that concerning the algorithm in Eq. (8) ranges from 0 GHz to 17 GHz. Clearly, the amplitude traces do not change when the frequencies are shifted. In Fig. 2(a), the traces are perfectly equal to that in Fig. 2(b) except for the frequency shift, as expected.

Figure 3 shows the three traces of the amplitude in TD derived by algorithms in Eqs. (3), (6), and (8). The three traces are perfectly overlapped, as expected. Note that the losses produce a gradual decay of the TD trace in time. The trace cannot be split in two part and representing them from $-T/2$ to $T/2$. The basic sequence transformed in TD is to be from 0 to T and not from $-T/2$ to $T/2$. It is included in the causality concept; it is also consistent with the reference plane termed by the calibration procedure.

Figure 4 shows details on the three traces of the TD phase concerning the algorithms in Eqs. (3), (6), and (8). The two traces of the phases concerning the algorithms in Eqs. (3) and (6) are perfectly

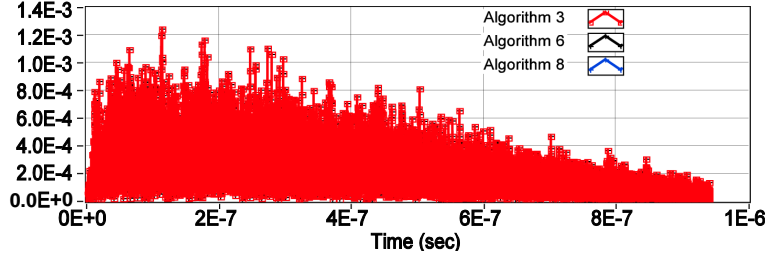


Figure 3. TD Amplitudes of the transmission coefficient measured in the RC and processed by algorithms in Eqs. (3), (6), and (8). The three traces are perfectly overlapped.

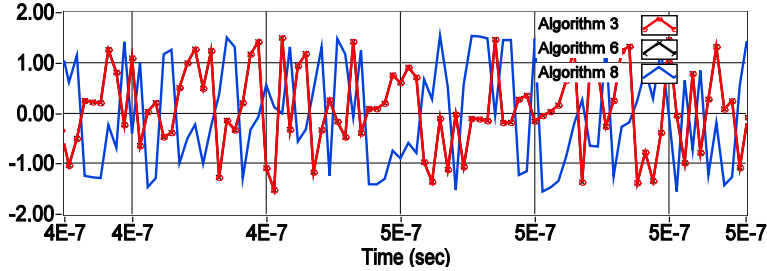


Figure 4. Details on the TD phases of the transmission coefficient measured in the RC and processed by the algorithms in Eqs. (3), (6), and (8). The two traces concerning the algorithms in Eqs. (3) and (6) are perfectly overlapped whereas that concerning the algorithm in Eq. (8) is different.

overlapped whereas the phase concerning the algorithm in Eq. (8) is different for the different shift in frequency.

Note that the same results are achieved by using the reflection parameters except for the well-visible mismatch of the antennas; they are not shown here to shortness. It is important to note that both TD traces and FD domain traces are in theory periodic from $-\infty$ to $+\infty$ [5, 7]. It is worth noting that the TD traces for bandpass frequency responses in VNAs [12–15] are represented from $-T$ to T by using a constant number of points (M ; M is equal to N). Strictly, the points corresponding to two periods ($2T$) are $2M$ [5, 7]. However, one must bear in mind that the causality has to be satisfied; it implies that the fundamental period in TD ranges from 0 to T . It should include M points even though mathematical manipulations are possible to change M . Note that the effect of the losses highlights the causality in TD, as shown in Fig. 3.

4. CONCLUSIONS

It is shown that the calculation of the IDFT for lowpass equivalent responses of passband frequency response measurements is obtained by two equivalent algorithms, which are denoted by Eqs. (3) and (6) in this paper. However, if only the amplitude of the complex envelope is requested, as is normally the case, we can use other algorithms as well; a special case is the algorithm in Eq. (8); such an algorithm is normally available in the common software such as MATLAB and LabVIEW. It is highlight that the TD complex responses derived from IDFT of lowpass equivalent responses are uniquely transformable in FD again; therefore, the algorithm in Eq. (8) can also be used every time that gating operations and a next DFT are to be applied to corresponding TD complex responses. It is also shown how the basic sequence has to be represented in time domain by invoking the causality, which is supported by results.

ACKNOWLEDGMENT

The Author thank Mr. Giuseppe Grassini of the Electrical and Electronic Measurements Lab (at Engineering Department, University of Napoli Parthenope) for his collaboration in the experimental work.

REFERENCES

1. Nicolson, A. M. and G. F. Ross, "Measurement of the intrinsic properties of materials by time-domain techniques," *IEEE Trans. on Instrum. and Meas.*, Vol. 19, No. 4, 377–382, Nov. 1970.
2. Hines, M. E. and H. E. Stinehelfer, "Time-domain oscillographic microwave network analysis using frequency-domain data," *IEEE Trans. on Microw. Theory and Techniques*, Vol. 22, No. 3, 276–282, Mar. 1974.
3. Ulriksson, B., "Conversion of frequency-domain data to the time domain," *Proc. of the IEEE*, Vol. 74, 74–77, 1986.
4. Papoulis, A., *The Fourier Integral and Its Applications*, Prentice-Hall, New Jersey, 1974.
5. Bracewell, R. M., *The Fourier Transform and Its Applications*, Prentice-Hall, New Jersey, 1974.
6. Carlson, A. B., *Communication Systems: An Introduction to Signal and Noise in Electrical Communication*, McGraw-Hill, New York, 1986.
7. Brigham, E. O., *The Fast Fourier Transform*, McGraw-Hill, New York, 1986.
8. Smith III, J. O., *Mathematics of the DFT with Audio Applications*, W3K Publishing, Stanford University, ISBN 978-0-97456007-4-8, Copyright 2014-04-21, 2007.
9. Holloway, C. L., H. A. Shah, R. J. Pirkl, K. A. Remely, D. A. Hill, and J. M. Ladbury, "Early time behaviour in reverberation chamber and its effect on the relationships between coherence bandwidth, channel decay time, RMS delay spread, and the chamber buildup time," *IEEE Trans. Electromagn. Compat.*, Vol. 54, 714–725, Aug. 2012.
10. Esposito, G., G. Gradoni, F. Moglie, and V. M. Primiani, "Stirrer performance of reverberation chambers evaluated by time domain fidelity," *IEEE Intern. Symp. on EMC*, 207–212, Denver, CO, USA, 2013, DOI: 10.1109/ISEMC.2013.6670410.
11. Zhang, X., M. Robinson, and I. D. Flintoft, "On measurement of reverberation chamber time constant and related curve fitting techniques," *IEEE Intern. Symp. on EMC*, 406–411, Dresden, Germany, 2015, DOI: 10.1109/ISEMC.2015.7256196.
12. Agilent Technologies, "Time domain analyzer using a network analyzer," Application note 1287-12, Literature number 5989-5723EN, Published in USA, May 2, 2012.
13. Hiebel, M., *Fundamentals of Vector Network Analysis*, Rhode & Schwarz, München, ISBN 978-3-939837-06-0, 2014.
14. Keysight Technologies, "Time domain analyzer using a network analyzer," Application note 1287-12, Literature number 5989-5723EN, Published in USA, Aug. 2, 2014.
15. Anritsu, "Time domain measurements using network analyzers," Application note No. 11410-00206, Rev. D, Printed in USA, 2009-03.
16. Campagnaro, G., "Private communication," Keysight Technologies, Italy, Mar. 2017.
17. Vaughan, R. G., N. L. Scott, and D. R. White, "The theory of bandpass sampling," *IEEE Trans. on Signal Processing*, Vol. 39, No. 9, 1973–1984, Sep. 1991.
18. Gifuni, A., A. Sorrentino, A. Fanti, G. Ferrara, M. Migliaccio, G. Mazarella, and F. Corona, "On the evaluation of the shielding effectiveness of an electrically large enclosure," *Advanced Electromagnetics*, Vol. 1, No. 1, 84–91, May 2012, DOI: <http://dx.doi.org/10.7716/aem.v1i1.44>.
19. Gifuni, A., G. Ferrara, M. Migliaccio, and A. Sorrentino, "Estimate of the shielding effectiveness of an electrically large enclosure made with pierced metallic plate in a well-stirred reverberation chamber," *Progress In Electromagnetics Research C*, Vol. 44, 133–144, 2013.
20. Migliaccio, M., G. Ferrara, A. Gifuni, A. Sorrentino, F. Colangelo, C. Ferone, R. Cioffi, and F. Messina, "Shielding effectiveness tests of low-cost civil engineering materials in a reverberating chamber," *Progress In Electromagnetics Research B*, Vol. 54, 227–243, 2013.